JOURNAL OF PROPULSION AND POWER
Vol. 23, No. 1, January–February 2007

Experimental and Theoretical Investigation of Base-Flow Buffeting on Ariane5 Launch Vehicles

Henry Wong*
Advanced Operations and Engineering Services and European Space Research and Technology Center, 2200 AG, Noordwijk, The Netherlands
Jos Meijer†
National Aerospace Laboratory, 1006 BM, Amsterdam, The Netherlands
and
Richard Schwane‡
European Space Research and Technology Center, 2200 AG, Noordwijk, The Netherlands

DOI: 10.2514/1.19740

A summary of some of the theoretical and experimental investigations of transonic base-flow buffeting on Ariane5 is described in this paper. The source and the mechanism of buffeting in the base flow, including its instability coupling with the local acoustic resonance, are identified and explained. A model for the Ariane5 base-flow buffeting is presented. Detailed comparisons between available experimental data and semiempirical predictions on the Ariane5 side-load resonant frequencies and amplitudes are highlighted. The main objective is to design a configuration for the Ariane5 base to have the base-flow buffeting on the Vulcain engine nozzle at least reduced, if not avoided.

Nomenclature

C_{SU}, C_{US}	=	scattering coefficients at the upstream and downstream ends of cavity
D	=	mean depth of cavity
f	=	frequency
L	=	length scale of cavity
M_∞	=	freestream Mach number
m	=	mode of instability
Re_t	=	turbulence Reynolds number
$Re[\alpha]$	=	ratio of freestream velocity and convective velocity of vortices
$Re[\tau_0^+]$	=	ratio of freestream velocity and phase speed of upstream propagating cavity mode of order zero
U	=	freestream velocity
X	=	downstream distance
ϕ	=	azimuthal angle
ω	=	angular frequency

I. Introduction

BASE-FLOW buffeting on Ariane5 has been identified as an important issue ever since the first launch of A501. Flight data recorded anomalous amplitudes of side loads acting on the Vulcain1 nozzle as a result of transonic base-flow buffeting. Extensive experimental and numerical research was conducted to assess the maximum side-load effect on Ariane5 [1,2]. The predicted side-load amplitude then turned out to be tolerable, as was demonstrated by all subsequent Ariane5 launchers. However, base-flow buffeting was again identified as a critical issue with respect to the launcher performance improvement in the area of propulsion. Large area-ratio nozzles, such as dual-bell nozzle or mechanical extendible nozzle, were proposed [3] that were more sensitive to the base-flow buffeting than the traditional nozzle because of a longer nozzle length, and consequently a larger moment about the fulcrum. In addition, base-flow buffeting could induce three-dimensional flow separation inside the nozzle [4]. Side loads on the nozzle could therefore be generated internally as well as externally as a result of a strong base-flow buffeting. For these reasons, a better understanding of how base-flow buffeting is initiated, amplified, and acoustically interfered, is considered desirable for future design in the nozzle. The main objective of this paper is to identify the source and the mechanism of buffeting in the base flow, including its instability coupling with the local acoustic resonance. It is our goal to design a configuration for the Ariane5 base to have the base-flow buffeting at least reduced, if not avoided. Studies of available experimental data and analytical modeling on base flow will also be addressed. A semiempirical model for the Ariane5 base-flow buffeting is proposed and compared with available experimental and flight data in terms of side-load resonant frequencies and amplitudes.

Presented as Paper 4548 at the 41st AIAA Joint Propulsion Conference and Exhibit, Tucson, Arizona, 10–13 July 2005; received 29 August 2005; revision received 3 May 2006; accepted for publication 19 May 2006.

*Senior Consultant; henry.wong@aoes.nl. Senior Member AIAA.
†Senior R&D Manager, Fluid Dynamics; meijer@nlr.nl.
‡Senior Engineer, Aerothermodynamics; Richard.Schwane@esa.int.

II. Theoretical Study for Steady Base Flow

Analytical modeling of steady base flow has been researched for many years in the past mainly because of its importance to aircraft design. It is worthwhile to mention the work by Baik and Zumwalt [5] who have developed a flow-modeling method to analyze the flow in the annular base (rear-facing surface) of a circular engine nacelle flying at subsonic speed but with a supersonic exhaust jet. Real gas properties and temperature are included. It is a steady axisymmetric model. The outer flow domain consists of the subsonic free shear layer and the supersonic jet from the nozzle. The inner flow consists of the domain enclosed by the free shear layer and the supersonic jet as shown in Fig. 1. Singularities are used for the inviscid subsonic airflow and the axisymmetric method of characteristics is used for the supersonic flow. Viscous boundary layers and viscous jet interactions are modeled by the Chapman–Korst jet mixing method.

The results can be summarized as follows:

1) The base pressure is lowered as the jet Mach number increases as shown in Fig. 2;

2) as the base pressure decreases, the jet-shear layer envelope shrinks and the shear layer comes closer to the nozzle as shown in Fig. 3;

3) as the boundary layer increases its thickness, the base pressure increases;

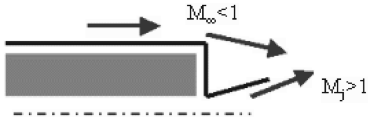

Fig. 1 Analytical model for base flow (Baik and Zumwalt).

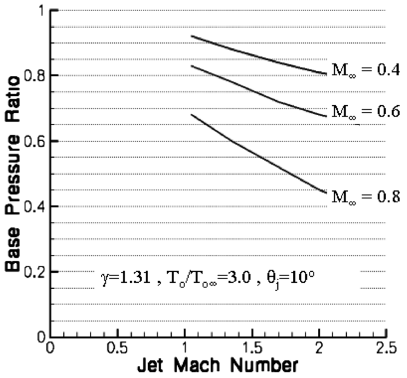

Fig. 2 Jet Mach number influence to base pressure (Baik and Zumwalt).

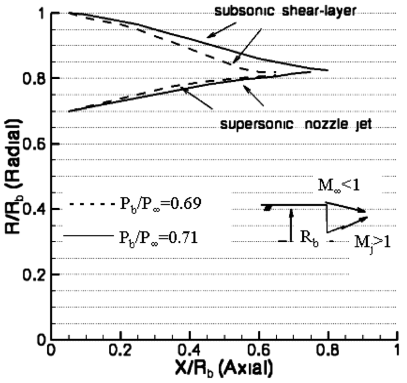

Fig. 3 Base pressure influence to jet and shear-layer envelope (Baik and Zumwalt).

4) as the jet nozzle deflection angle increases, the base pressure increases.

Similar results have been achieved by Dixon et al. [6] who have analyzed turbulent base flow on an axisymmetric body with a single exhaust jet by extending Korst's two-stream theoretical base-flow analysis. However, the freestream in this case is supersonic with turbulent axisymmetric mixing occurring along the separated flow boundaries.

It can be concluded from these results that the jet Mach number has a significant influence on the envelope enclosed by the supersonic jet and the subsonic shear layer. Moreover, the higher the jet Mach number is, the closer the shear layer approaches to the nozzle. Based on the consideration of the base-flow pressure distribution, the boundary layer thickness, the base geometry, and the Mach numbers, this conclusion is valid for the Ariane5 base flow. It may be not valid for other configurations and different flow conditions such as missiles or launchers with a cluster of nozzles. However, there is still one remaining source of uncertainty associated with the Ariane5 shear-layer envelope. If the shear layer reattaches, or impinges on or near the nozzle, before it recoils and interacts with the jet, then it is not necessarily correct that the shear-layer envelope shrinks when the jet is turned on. Some of these results will be compared with the experimental data described in the experimental study section.

III. Ariane5 Base-Flow Buffeting Model

It is assumed that the main source of base-flow buffeting is instability of the free shear layer emanating from the edge of the central body below the launcher central cryogenic engine (EPC). This kind of shear-layer instability, similar to Kelvin–Helmholtz instability, interacts with the upstream propagating acoustic waves, generated by the impingement of the vortices associated with the shear layer, along the external surface of the EPC Vulcain engine nozzle downstream. This interaction amplifies the instability of the shear layer resulting in the shedding of new vortices or oscillatory waves, and possibly an amplitude increase in the shear-layer excitation. In this way, the vortices or oscillatory waves and the acoustic disturbances form a feedback loop. Based on this hypothesis, which is similar to the Rossiter [7] model for rectangular cavities, the base-flow domain of Ariane5 is modeled by a rectangular cavity with the same L/D ratio as shown in Fig. 4. L is the distance the shear layer propagates from the edge of the central body EPC to the EPC nozzle downstream, and D is the mean depth between the shear layer and the external solid surface of the Ariane5 base structure that consists of the propulsion module (PTM) and the Vulcain nozzle. The L/D ratio for the Ariane5 configuration is approximately 8.5. The main components of the acoustic waves induced by the shear-layer instability are indicated in Fig. 4. The shear layer can deflect upward and downward relative to the trailing edge of the cavity during its oscillatory movement over the cavity. The compression wave front EE' is mainly induced by the impingement of an inflow from the external fluid M_∞ on the trailing edge of the cavity when the shear layer is deflecting downward. The waves $B'B''$ and $A'A''$ are caused by the reflections at the bottom wall and the upstream end wall, respectively. According to Tam and Block [8], the acoustic wave $A'A''$ is the most important wave to excite the instability waves of the shear layer.

Kerschen and Tumin [9] presented an analytical model based on edge scattering processes coupled with a linear instability theory to yield the Rossiter semiempirical formula as

$$\frac{\omega L}{U} = 2\pi \frac{m - (\arg[C_{SU}] + \arg[C_{US}])/2\pi}{Re[\alpha + \tau_0^+]} \tag{1}$$

The left-hand side of the equation is basically the Strouhal number. On the right-hand side of the equation, the scattering coefficients on the numerator are determined by a vortex-sheet approximation. A liplike geometry with a finite length overhanging at each end of the cavity is considered. The acoustic field satisfies the no-penetration boundary condition at the bottom of the cavity and matches the continuity conditions for the pressure and displacement across the vortex sheet. At the downstream end of the cavity, the incident field is the shear-layer instability wave which can be analyzed by the triple decomposition method similar to the one employed by Yang and Tumin [10]. The effect of the shear-layer instability wave is reflected in the denominator on the right-hand side of Eq. (1). The evolution of

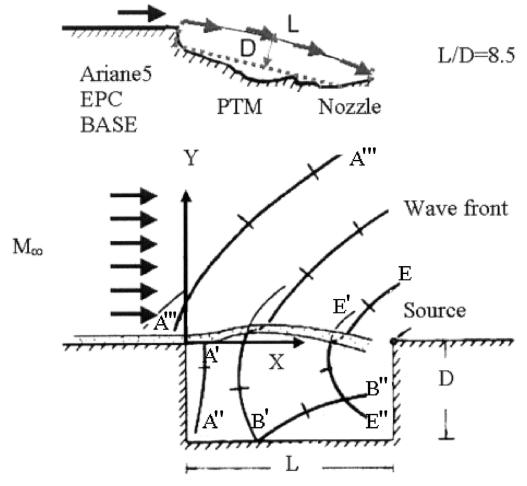

Fig. 4 Ariane5 base-flow buffeting model.

the acoustic cavity mode propagating through the length of the cavity is analyzed in a similar fashion except that the mode is extended across the depth of the cavity instead of transmitted through the thickness of the shear layer.

Equation (1) was validated [7,9] in the past mainly for the Mach range 0.4–1.2. There were many researchers [11–13] for the last three decades modifying the original Rossiter's semiempirical formula to extend its validity outside the specified Mach number range. For very low subsonic flow, $M_\infty < 0.2$, the tones were generated by normal mode resonance mechanism rather than by the feedback mechanism mentioned above. The critical range of Mach numbers for the Ariane5 base-flow buffeting investigation was from 0.5 to 0.95 within the Rossiter's validated Mach range.

Figure 5 shows a general example of the global dispersion relation in the complex frequency plane. There are four global instability modes shown in which only the first three modes are temporally unstable. The second mode has the largest temporal growth rate and the third mode has the smallest. The L/D ratio is 4 with a freestream Mach number 1.2. Assuming the general hypothesis in the research of linear instability that the strongest temporal growth rate leads to the largest nonlinear resonant amplitude, this result is consistent with Rossiter's experimental data both in the number of unstable modes ($m = 1$, 2, and 3) and the relative amplitudes of these modes as shown in Fig. 6. Figure 6 shows a comparison in the Strouhal numbers of the instability modes between the theoretical prediction and the experimental data. Based on the consideration of the scattering coefficients, the convective velocity of vortices and the Rossiter's data, Ariane5 with a ratio of $L/D \cong 8.5$ is predicted to have a Strouhal number of $\cong 0.2$ for the first unstable mode. The strongest temporal growth rate takes place in the second unstable mode corresponding to a Strouhal number of $\cong 0.55$. According to the flight dimension of Ariane5, the first and second unstable modes are therefore predicted to take place at 6 ± 1 Hz and 15 ± 2 Hz, respectively.

The resonant amplitude cannot be analyzed by the linear instability theory. However, it can be estimated by the triple decomposition solution of compressible mixing layers by Yang and Tumin [10]. Figure 7 shows the amplification of the pressure disturbance, including the nonparallel flow effects, of a spatially developing shear layer as a function of the downstream distance X, normalized by a length scale corresponding to the peak of the amplification for the case Mach 0.6 with a Re_t 16.6. The plot shows the two extreme cases in amplification where the inviscid case with a higher turbulence Reynolds number is amplified 3 or 4 times more than the case with a lower turbulence Reynolds number where strong interactions exist between coherent and random disturbances. The inviscid case is approximately for a deep cavity, and the other case is for a shallow cavity. For the Ariane5 configuration, the turbulence Reynolds number of the shear layer is strongly influenced by the upstream boundary layer thickness, the freestream Mach number, and the dimensions of the cavity. Ariane5 has a long central body with a Reynolds number of 10^9 at Mach 0.8. The flow at the base is fully turbulent. However, the base configuration of Ariane5, modeled by an axisymmetric cavity with the ratio $L/D \cong 8.5$ as shown above, is classified as a shallow cavity. Moreover, the mode of oscillation as shown by Shieh and Morris [14] for a three-dimensional cavity is a shear-layer type satisfying the theory of Yang and Tumin and can be predicted by Eq. (1). It is therefore reasonable to assume that the turbulence Reynolds number, which is proportional to the ratio of the eddy viscosity and the dynamic viscosity, is close to the shallow cavity case for the Ariane5 configuration.

Based on the above consideration, at Mach 0.8, the maximum amplification of pressure fluctuations is predicted to be not larger than 13 times according to the data in Fig. 7. Nevertheless, there are some uncertainties in this estimation. Colonius et al. [15] using direct numerical simulation have demonstrated that in two-dimensional cavities the increase in L/D leads to transitions from a shear-layer mode to a wake mode of oscillations. It is not known exactly whether this applies to three-dimensional cavities or not. In addition, the maximum amplification factor is assumed to be governed mainly by

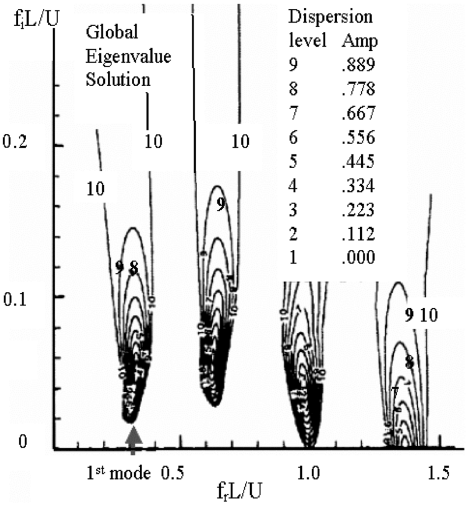

Fig. 5 Global dispersion relation in a complex frequency plane (Kerschen and Tumin).

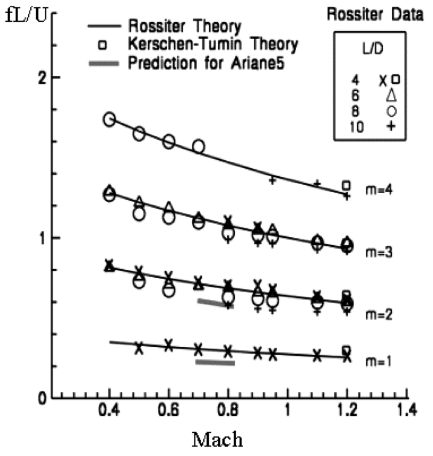

Fig. 6 Comparison between Rossiter's experimental data (1964) and the theory of Kerschen and Tumin (2003).

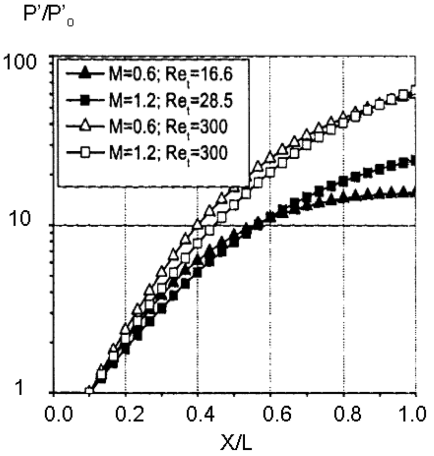

Fig. 7 Amplification of pressure fluctuations along the downstream distance of a spatially developing shear layer (Yang and Tumin [10]).

the shear-layer instability. As mentioned above in the Ariane5 base modeling, the acoustic waves across the shear layer downstream are assumed to have secondary effects on the maximum amplification factor, despite the fact that the acoustic resonance supports and augments this instability through the receptivity process at the upstream end of the cavity. Another uncertainty comes from the

relatively simple modeling of a Newtonian eddy viscosity in the theory of Yang and Tumin for the interaction between coherent and random disturbances. Reau and Tumin [16] have claimed that the theory agrees with the experimental data and has been independently supported by Gaster et al. [17] in their research. Further discussion of the effect on the shear-layer instability from the wake mode of oscillations and the normal mode of resonance, which are usually associated with a deep cavity, will not be addressed in this paper. Comparison between the theory and the experimental data in the resonant frequencies and the amplification factor is shown below.

IV. Experimental Data Investigation

The experimental data for this investigation are based on the available documented [1] data from the PHST wind tunnel in the National Aerospace Laboratory (NLR) and the T1500 wind tunnel in the Swedish Defense Research Agency (FOI). Some of the documented [1] data are extracted from the wind tunnel S2 Modane in the French National Aerospace Research Establishment (ONERA) for comparison with the data from the other wind tunnels. These experiments were conducted between 1996 and 1997 after the first Ariane5 flight (V501) using a 1:76.5 subscale Ariane5 model. By adjusting the length of the model, the ratio of the boundary layer thickness at the edge of EPC to its diameter was around 1.7 times larger in the wind tunnel than in the flight. The Reynolds number for the model, based on the streamwise length scale, was on the order of 10^7. The base flow was fully turbulent in the model just as in the flight. Cold, pressurized nitrogen was used as the exhaust gas through the nozzle and the two boosters. The nozzle was designed to duplicate the outflow angle of the plume in flight with the exit Mach number and the Prandtl–Meyer expansion as the main mechanisms. Goethert scaling rules were imposed as a first guideline in the design. The plume stiffness and the static pressure ratio were considered secondary effects.

Based on the theoretical study mentioned above, it can be seen that a good decision has been made in the nozzle design to match the outflow angle of the plume, and the adjustment for a more appropriate upstream boundary layer thickness is important. However, the incorrect static pressure at the outflow could affect somewhat the impingement of the shear layer on the nozzle. The freestream Mach number ranges from 0.4 to 0.9. More than 40 Kulites were distributed uniformly over the Ariane5 base for measurements as shown in Fig. 11. Low and high fan speeds were taken into account for the assessment of the wind tunnel interference. The experiments were conducted to examine the following effects on nozzle side loads: 1) geometrical effects (protuberances, exhaust pipes, skirt, splitter plates, and rods), 2) jet on and off, 3) yaw angle, 4) incidence angle.

To minimize statistical errors on the experimental data, the duration of measurement at each Kulite was long (a few seconds) and accurate enough to resolve a differential frequency of 10 Hz out of a 1000 Hz with the subscale model testing conditions.

The results from those tests helped to better characterize the side-load sensitivity to these variables. However, the underlying mechanism governing nozzle buffeting was not understood. There was no explanatory theory at that time and all efforts were concentrated on the effect rather than on the cause. The current research has revisited the experimental data again attempting to understand better what physical mechanism the data have indicated.

First, let us start with the mean flow through the mean pressure distribution at various Mach numbers as shown in Fig. 8. It can be seen at all Mach numbers that the mean pressure is lower when the jet is on than when it is off. This is consistent to what the theory predicts. The low static pressure from the jet envelope has a strong suction effect on the base pressure. As a result, the shear-layer envelope shrinks and impinges or reattaches at a location further upstream along or near the nozzle. The mean pressure distribution also indicates that the mean pressure is higher at P1 and P2 downstream than at P3 and P4 upstream independent of the jet on or off. This could indicate that the shear layer has already reattached or impinged on, or just come close to, the nozzle before the jet is turned on. This

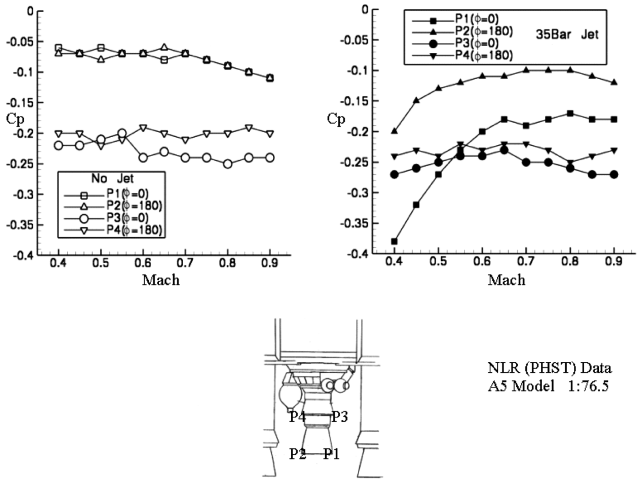

Fig. 8 Mean pressure distribution along PTM and the nozzle at various Mach numbers.

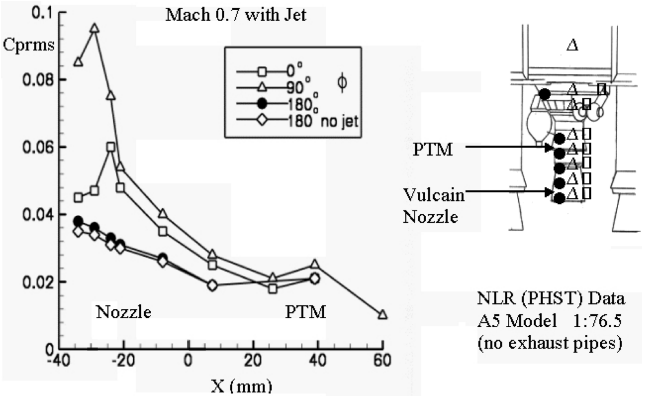

Fig. 9 Distributions of pressure fluctuations along PTM and the nozzle at different azimuthal angles.

flow phenomenon can be understood better as we further examine the distribution of pressure fluctuations along the nozzle.

We begin to investigate the unsteady phenomena from the distribution of the pressure fluctuations along the PTM and the nozzle as shown in Fig. 9. There are three different profiles corresponding to the azimuthal angles of 0 (right), 90 (center), and 180 (left) deg. The characteristics of these profiles are very similar at all the Mach numbers tested (0.5–0.9). The peak in the $\phi = 0$ deg profile indicates that the shear layer could have reattached or impinged on, or come close to and recoiled from, the nozzle surface at some distance upstream from the nozzle exit. The $\phi = 180$ deg profile without a peak indicates that the shear layer could have impinged onto the jet directly. This difference in the impingement location could be attributed to the influence of the protuberance from the helium tank. Similar profiles are shown in the case without jet except that the $\phi = 180$ deg profile shifts lower at the location near the nozzle exit, indicating that the shear layer has drifted further away from the nozzle. The $\phi = 0$ deg profile remains almost the same as in the case with the jet turned on. The $\phi = 180$ deg profile interacting directly with the jet agrees with the theory but the effect is not significant. Further experimental evidence is required to confirm this conclusion.

Perhaps the most important information in the figure is the $\phi =$ 90 deg profile which shows a much larger pressure fluctuation compared with the other profiles. The maximum amplification of the pressure fluctuations is around 10 compared to the upper bound estimation of a factor of 13 by the theory of Yang and Tumin. Similar pressure fluctuations along the PTM and the nozzle at various azimuthal angles have been measured by different wind tunnels at NLR, FOI, and ONERA research centers with different freestream Mach numbers as shown in Fig. 10. The pressure fluctuations in the Z

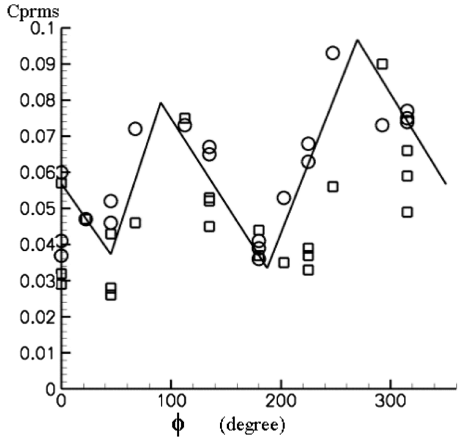

Fig. 10 Pressure fluctuations around the nozzle exit at various azimuthal angles with different Mach numbers. □: M0.9, and ○: M0.5.

direction ($\phi = 90$ deg and $\phi = 270$ deg plane) are much larger than those in the other ϕ angles as indicated by the solid lines. However, does this imply that the side load on the nozzle is dominant in this direction? It is not possible to answer this question without first finding out the relative phases between the pressure fluctuations around the nozzle.

Based on the cross correlation and coherence functions between different Kulites, and cross checked with their corresponding cross-power spectra, the relative phases between the pressure fluctuations at different locations around the nozzle within the frequency range of 5 to 15 Hz can be summarized as shown in Fig. 11. Similar phase distributions have been measured from Mach 0.6 to Mach 0.8. Three cross sections of the nozzle are shown with the top curve corresponding to the top cross section as indicated by the arrows. It can be seen that the relative phases between the pressure fluctuations (pairs of Kulites K3, K5 and K2, K6) in the Z direction ($\phi = 90$ deg and $\phi = 270$ deg plane) are almost in phase with a 20 deg phase shift. However, in the Y direction ($\phi = 0$ deg and $\phi = 180$ deg plane), the phase shift (pairs of Kulites K1, K4 and K7, K10 and K13, K15) is around 120 deg. For this reason, the integrated force in the $\phi = 90$ deg and 270 deg plane (Z direction) is predicted to be less than that in the $\phi = 0$ deg and 180 deg plane (Y direction).

The integrated forces from the experiments with a high fan speed at Mach numbers 0.7 and 0.8 are shown in Fig. 12. The relative magnitudes between the integrated forces in the Y and Z directions agree with the prediction. Similar behavior in the case with a low fan speed at Mach 0.8 is shown later. The influence of the wind tunnel interference is more significant at Mach numbers lower than 0.7 as mentioned by Meijer and van Beek [1]. This may explain the relatively large peak in the Y integrated force for the first mode resonant frequency at Mach 0.7 in Fig. 12. Figure 12 also shows that

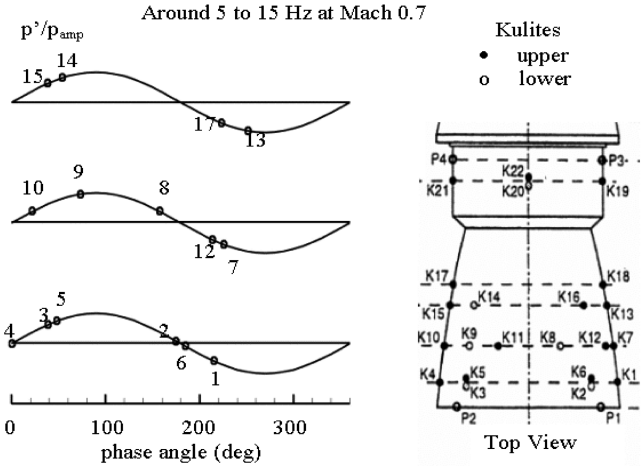

Fig. 11 Relative phases between pressure fluctuations at different locations around the nozzle.

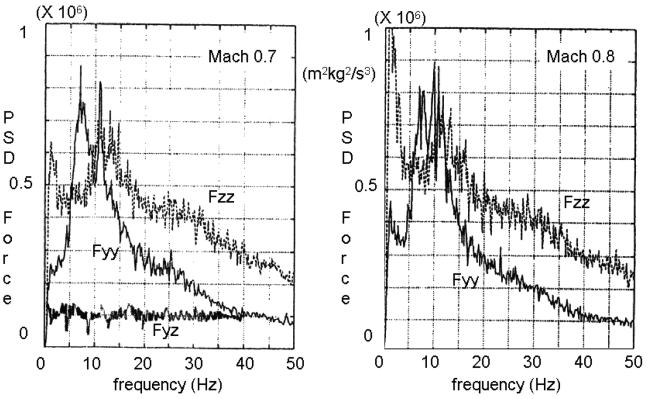

Fig. 12 Integrated forces at Mach 0.7 and Mach 0.8 (high fan speed) with jet.

the cross-power spectral density of the Y and Z forces is relatively weak compared to the power spectral density of each individual force. This supports the application of the Rossiter two-dimensional theory that the unsteady force in each direction behaves approximately independent of each other. Experiment shows good agreement with theory in that the resonant frequencies have been measured as 6–7 Hz and 10–12 Hz for the first and second Rossiter modes, respectively. According to the documented flight data [18], the largest amplitude in the side load on the nozzle takes place at a frequency of around 10 Hz. Moreover, the second mode in the experiment yields the largest integrated force in the Y direction, and is the most unstable mode as predicted by the theory. It is harder to show the resonant force in the Z direction because of the small differences in the relative phases between the two opposite sides. The results shown in Fig. 12 are based on a configuration with two exhaust pipes attached to the external surface of the nozzle in the plane $Y = 0$. This is similar to the Vulcain1 model in the flight configuration as shown in Fig. 13. The effect of the exhaust pipes on the integrated forces is mainly in the Y direction as shown in Fig. 14. The sharp peaks of the integrated forces at the resonant frequencies have been attenuated significantly without the exhaust pipes. The absence of the exhaust pipes attached to the nozzle effectively increases the depth of the cavity and consequently diffuses the impact of the impingement of the shear layer on or close to the nozzle. This could explain the attenuation of the integrated force in the Y direction as shown in Fig. 14. The effect of the jet on the integrated force is not significant as already explained in the distribution of the pressure fluctuations along the nozzle. The effect of no protuberance (without the helium tank) is shown in Fig. 15. Without the helium tank the launcher configuration is symmetric in both the Y and the Z directions; as a result the sharp peaks of the integrated forces at the resonant frequencies have been attenuated significantly. The magnitude of the integrated force in the Y direction ($\phi = 0$ deg and 180 deg plane) is in this case smaller than that in the Z direction ($\phi = 90$ deg and 270 deg plane). This agrees with the prediction by the pressure fluctuation distribution along the nozzle as shown in Fig. 9. However, an additional unknown resonant force at a higher

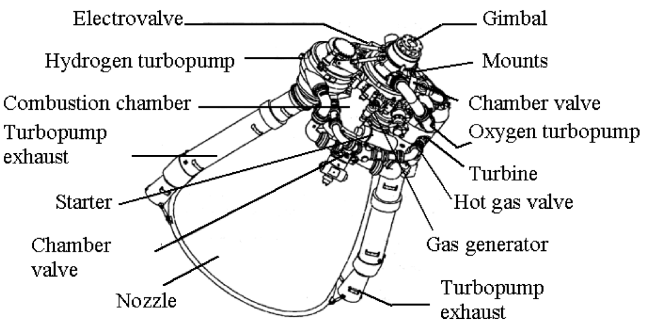

Fig. 13 An example of the nozzle flight configuration with exhaust pipes.

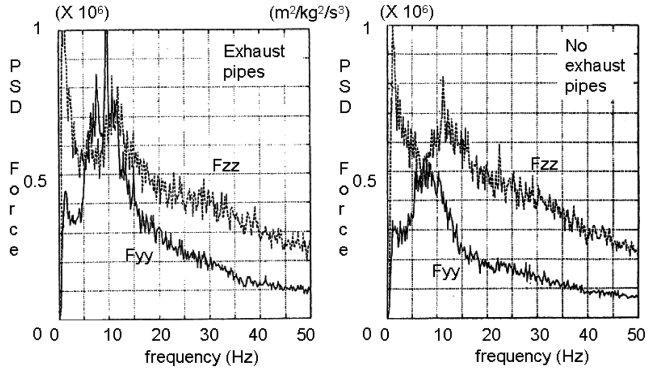

Fig. 14 Integrated forces at Mach 0.8 (low fan speed) with jet, with (left) and without (right) exhaust pipes attached to the nozzle.

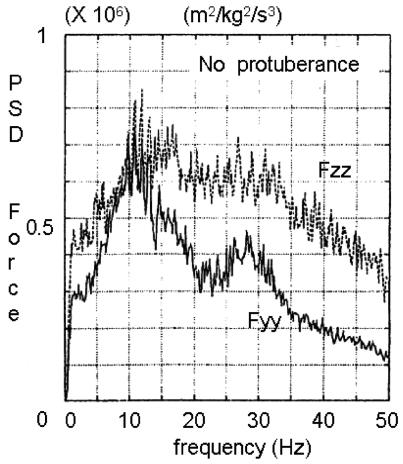

Fig. 15 Integrated forces with no protuberance at Mach 0.8.

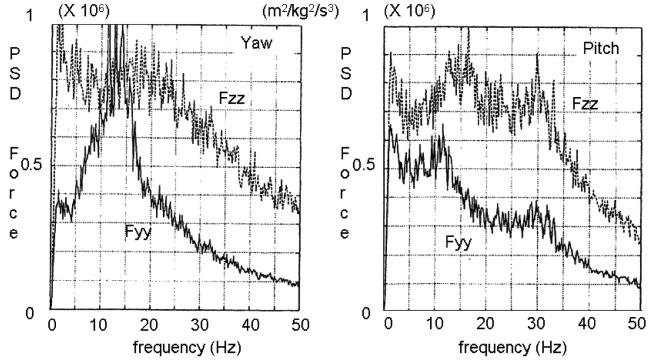

Fig. 16 Influence of 5 deg yaw (left) and 5 deg pitch (right) to integrated forces at Mach 0.8 with jet but without exhaust pipes.

frequency is generated, particularly in the Y direction. These resonant forces are most likely originated from the wakes mode rather than from the shear-layer mode of oscillations in the base flow. We shall not discuss this unknown resonant force further here.

Figure 16 shows the influence of the aerodynamic yaw and pitch to the resonant forces in the Ariane5 experimental model at Mach 0.8 with jet but without the exhaust pipes attached to the nozzle. A 5-deg yaw angle relative to the $Y = 0$ plane (refer to Fig. 8) and, independently, a 5-deg pitch angle relative to the $Z = 0$ plane have been simulated by the experiment. The integrated forces in Fig. 16 can be compared with those in Fig. 14 (right); it can be seen that the resonant forces in both directions have been amplified significantly. The integrated force in the Y direction is more sensitive to the yaw than to the pitch effect. The combination of all the physical effects mentioned above, mainly the yaw and the pitch, the exhaust pipes and the helium tank protuberance, renders a large side-load effect on the nozzle as reported in the flight data.

V. Conclusion

A summary of theoretical and experimental investigations of transonic base-flow buffeting in the Ariane5 launcher is given. It is shown that a model, based on shear-layer instability and augmented by acoustic resonance, for the Ariane5 base-flow buffeting can explain the major aeroacoustic phenomena that exist in the base-flow domain of Ariane5. Resonant frequencies and amplitudes are in good agreement with the experimental data. Further experimental and flight data and numerical investigations will be necessary to confirm these results.

This is a milestone that brings us a step closer to understand and resolve the complicated and important aeroacoustic phenomena beneath the powerful Ariane5 launcher. Only with a deeper acquaintance and understanding of these phenomena can we design and improve the launcher propulsion efficiency in the future by reducing the base-flow buffeting effect on the launcher.

Acknowledgments

The authors gratefully acknowledge the support and encouragement from the colleagues in the European Space Technology and Research Center, especially Jean Muylaert and Wilhelm Kordulla. A part of this work has been performed within the framework of the European Flow Separation Control Device (FSCD) Working Group. The authors are deeply indebted to the FSCD colleagues for many fruitful discussions and valuable comments.

References

[1] Meijer, J. J., and van Beek, C. M., "Analysis of Ariane5 Base Flow Measurements in the NLR/PHST and FFA/T1500 Wind Tunnels," National Aerospace Laboratory, NLR-CR-99449, Nov. 1999.

[2] Wong, H., and Schwane, R., "Final Report on Numerical Support to Aerodynamics Buffeting Problems in Ariane5," European Space Technology and Research Centre, Doc. YPA/2236/HW, Aug. 1997.

[3] Hagemann, G., Preuss, A., Grauer, F., Frey, M., Kretschmer, J., Ryden, R., Jensen, K., Stark, R., and Zerjeski, D., "Flow Separation and Heat Transfer in High Area-Ratio Nozzles," *40th AIAA Joint Propulsion Conference and Exhibit*, AIAA, Reston, VA, July 2004, pp. 1–8; also AIAA Paper 2004-3684.

[4] Wong, H., "A Brief Overview on Some Resonance Phenomena in Nozzle Flows," *40th AIAA Joint Propulsion Conference and Exhibit*, AIAA, Reston, VA, July 2004, pp. 1–26; also AIAA Paper 2004-4013.

[5] Baik, D. S., and Zumwalt, G. W., "Analytical Model of the Base Flow Between a Subsonic and Supersonic Flow," *Journal of Propulsion and Power*, Vol. 18, No. 1, 2002, pp. 35–43.

[6] Dixon, R. J., Richardson, J. M., and Page, R. H., "Turbulent Base Flow on an Axisymmetric Body with a Single Exhaust Jet," *Journal of Spacecraft and Rockets*, Vol. 7, No. 7, 1970, pp. 848–854.

[7] Rossiter, J. E., "Wind Tunnel Experiments of the Flow over Rectangular Cavities at Subsonic and Transonic Speeds," Royal Aircraft Establishment, TR No. 64307, Oct. 1964.

[8] Tam, C. K. W., and Block, P. J. W., "On the Tones and Pressure Oscillations Induced by Flow over Rectangular Cavities," *Journal of Fluid Mechanics*, Vol. 89, No. 2, 1978, pp. 373–399.

[9] Kerschen, E. J., and Tumin, A., "A Theoretical Model of Cavity Acoustic Resonances Based on Edge Scattering Processes," *41st Aerospace Sciences Meeting and Exhibit*, AIAA, Reston, VA, Jan. 2003, pp. 1–10; also AIAA Paper 2003-175.

[10] Yang, H., and Tumin, A., "On Harmonic Perturbations in Compressible Mixing Layers," *32nd AIAA Fluid Dynamics Conference and Exhibit*, AIAA, Reston, VA, June 2002, pp. 1–11; AIAA Paper 2002-2854, .

[11] Block, P., "Noise Response of Cavities of Varying Dimensions at Subsonic Speeds," NASA TN D-8351, 1976.

[12] Bilanin, A., and Covert, E., "Estimation of Possible Excitation Frequencies for Shallow Rectangular Cavities," *AIAA Journal*, Vol. 11, No. 3, 1973, pp. 347–351.

[13] Heller, H., and Bliss, D., "The Physical Mechanism of Flow Induced Pressure Fluctuations in Cavities and Concepts for Suppression," AIAA Paper 1975-0491, March 1975.

[14] Shieh, C. M., and Morris, P. J., "Comparison of Two Dimensional and

Three Dimensional Turbulent Cavity Flows," AIAA Paper 2001-0511, 2001.
[15] Colonius, T., Basu, A. J., and Rowley, C. W., "Numerical Investigation of the Flow past a Cavity," AIAA Paper 99-1912, 1999.
[16] Reau, N., and Tumin, A., "On Harmonic Perturbations in Turbulent Wakes," *AIAA Journal*, Vol. 40, No. 3, 2002, pp. 526–530.
[17] Gaster, M., Kit, E., and Wygnanski, I., "Large Scale Structures in a Forced Turbulent Mixing Layer," *Journal of Fluid Mechanics*, Vol. 150, No. 2, Jan. 1985, pp. 23–39.
[18] Radulovic, S., "Synthese des Essais "Buffeting"—Comparison avec les Vols. 501 et 502," Centre National D'etudes Spatiales, DLA-NT-0-385-CNES, 1998.

T. Wang
Associate Editor